Journal of Environmental Informatics 43(1) 16-30 (2024)

Journal of Environmental Informatics

www.iseis.org/jei

Recent Advances in Constructing Three-Dimensional Graphitic Carbon Nitride Based Materials and Their Applications in Environmental Photocatalysis, Photo-Electrochemistry, and Electrochemistry

W. Xia[1], X. Li[1], M. Cheng[1], W. P. Xiong[1], B. Song[1], Y. Liu[1], Y. Yang[1], W. J. Wang[1], S. Chen[1], G. M. Zeng[1 *], and C. Y. Zhou[1 *]

[1] *College of Environmental Science and Engineering, Hunan University and Key Laboratory of Environmental Biology and Pollution Control (Hunan University), Ministry of Education, Changsha 410082, P.R. China*

Received 03 September 2020; revised 20 February 2021; accepted 28 May 2021; published online 05 January 2024

ABSTRACT. Recently, graphitic carbon nitride (g-C_3N_4), a promising visible-light-driven semiconductor material, has received enormous attention for photocatalytic water splitting, organic pollutant degradation, and CO_2 reduction. However, the photocatalytic activity of bulk g-C_3N_4 is restricted due to the insufficient light adsorption, ineffective utilization of photogenerated charge carriers, and low specific surface area. Compared with bulk g-C_3N_4, the three-dimensional graphitic carbon nitride based materials (3D CNBMs) have outstanding physical and chemical characteristics, such as large specific area, plentiful active sites, and excellent electrical conductivity. This article reviews the latest achievements in 3D CNBMs, and presents the state-of-the-art advances in the synthetic methods of 3D CNBMs. Meanwhile, various applications of 3D CNBMs in photocatalysis, photo-electrochemistry, and electrochemistry are systematically reviewed and discussed. In addition, possible improvements and perspectives of 3D CNBMs are proposed. This review aims to summarize a panorama of the up-to-date processes of 3D CNBMs in environmental and energy applications and provide some innovative thoughts to accelerate the ground-breaking research and development of 3D CNBMs for a sustainable future.

Keywords: environmental or energy applications, g-C_3N_4, photo-electrochemistry, synthetic methods, three-dimensional

1. Introduction

Human beings rely heavily on fossil fuels like petroleum, coal, and natural gas in modern society, making environmental pollution, and energy shortage become the two most prominent global issues at present (Huang et al., 2019; Ji et al., 2020; Qin et al., 2020; Xie et al., 2020; Xing et al., 2020; Ye et al., 2020; Zhou et al., 2020d). Environmental protection and renewable energy development have become the key to the sustainable development of mankind. Photocatalysis technology, which can directly take advantage of solar energy, has the characteristics of mild reaction, low energy consumption, and no secondary pollution (Cheng et al., 2019; Ye et al., 2019; Zhao et al., 2019; Li et al., 2020; Wu et al., 2020). It is of great significance and practical research value to commercialize the photocatalysis technology in environmental remediation and energy conversion (Wang et al., 2014; Zhou et al., 2019b; He et al., 2020).

At present, conventional photocatalyst materials can be divided into single-component inorganic semiconductor photocatalysts (Nakamura et al., 2000; Scuderi et al., 2016; Di Mauro et al., 2017;), composite photocatalysts (Wang et al., 2016b; Golestanbagh et al., 2018), and metal photocatalysts (Sakthivel et al., 2004; Li et al., 2016; Cao et al., 2017). Inorganic semiconductor photocatalysts refer to metal oxides, metal sulfides, etc. Titanium dioxide (TiO_2) is extensively studied owing to its chemical stability, non-toxicity, and low price (Zheng et al., 2010; Shi et al., 2019; Luo et al., 2020; Wang et al., 2020a). However, the application of TiO_2 is limited due to its wide bandgap (3.0 ~ 3.2 eV over different phases). It can only absorb ultraviolet light accounting for a very low proportion of the sunlight, resulting in the low utilization of solar energy (Silva et al., 2011; Yan et al., 2017a). Cadmium sulfide (CdS), as a kind of metal sulfide photocatalysts, has become a high performance photocatalyst material with wide wavelength absorption range and good carriers transportation capacity (Zhang et al., 2014b; Cheng et al., 2018). However, the chemical stability of CdS is poor. In the photocatalytic process, sulfur ion is easy to be oxidized by holes, which causes the simultaneous release of Cd(II) into the system and then resultes in environmental pollution (He et al., 2017). Usually, two or more inorganic semiconductor materials are connected to form composite photocatalysts. Since the energy band structures of semiconductor materials are different, the composite photocatalyst can overcome the disadvantages of the low utilization rate of sunlight of single semiconductor materials (Huang et al., 2020a). Metal photocatalysts can be divided into photo-

* Corresponding author. Tel.: +86 731-88822754; fax: +86 731-88823701.
E-mail address: zgming@hnu.edu.cn (G. M. Zeng).
* Corresponding author. Tel.: +86 731-88822754; fax: +86 731-88823701.
E-mail address: zhouchengyun@hnu.edu.cn (C. Y. Zhou).

ISSN: 2663-6859 print/2663-6867 online
 doi:10.3808/jei.202400505.

catalysts containing a single metal element and heteronuclear complex photocatalysts composed of two metals (e.g., Ru-Pd, Ru-Rh, etc) (Duan et al., 2020). Bismuth (Bi) is a heavy metal with low-radioactivity and low-toxicity. It is abundant on earth, only second to silver. It has a good development prospect in the fields of medicine, organic synthesis, and catalysis. In the field of photocatalysis, most Bi-based photocatalysts are Bi(III) oxides, such as BiOCl, BiOBr, BiOI, Bi_2WO_6, $BiPO_4$, Bi_2O_3, $BiVO_4$, etc (Jiang et al., 2010; Ge et al., 2011; Ye et al., 2014; Li et al., 2018a; Sánchez-Rodríguez et al., 2018; Yi et al., 2019; Wang et al., 2020c). However, the poor utilization of visible light and the fast recombination of electron-hole pairs lead to unsatisfied photocatalytic performance (He et al., 2018b). Single-component silver-based semiconductor has high absorptivity to visible light and shows good catalytic activity in photocatalytic applications. Nevertheless, their poor stability and high price limit their practical applications (Huang et al., 2020b; Xue et al., 2020).

Wang et al. (2009a) successfully synthesized graphitic carbon nitride (g-C_3N_4), a non-metal conjugate semiconductor composed of nitrogen and carbon elements, which could split water into hydrogen and oxygen after absorbing visible light. Graphitic carbon nitride has the advantage of distinguished energy band, remarkable physicochemical stability, facile synthesis, and environmental friendliness (Ong et al., 2016; Yang et al., 2020b). Specifically, it has a graphene-like planar structure, which composed of tri-s-triazine units by deamination. The bandgap of g-C_3N_4 (2.7 eV) is narrower than that of TiO_2, which means that g-C_3N_4 can utilize part of visible light in the photocatalytic reactions. Furthermore, g-C_3N_4 has high heat-resistance and can stably exist in acid and alkali conditions. It can be simply fabricated by thermal polymerization with economical nitrogen-riched precursors (such as dicyandiamide, thiourea, melamine and urea) (Yan et al., 2009; Yang et al., 2020d). However, bulk g-C_3N_4 usually shows unsatisfied photocatalytic performance owing to its low specific surface area, insufficient absorption to solar energy, and high possibility of recombination of photo-electron-hole (Zhang et al., 2016b; Khan et al., 2018; Yang et al., 2019; Wang et al., 2020a).

In order to enhance the photocatalytic activity of g-C_3N_4, researchers have carried out extensive studies. The modification methods mainly include element doping (Wang et al., 2009b; Zhang et al., 2014a; Wang et al., 2015a; Zhou et al., 2020b), heterojunction construction (Dong et al., 2013; Li et al., 2017) and morphological control (Yang et al., 2015; Shakeel et al., 2019; Wang et al., 2021a). Element doping is to control the energy band structure of g-C_3N_4 by doping with homo-elements or hetero-elements. It can be divided into metal doping and non-metal doping. When metal elements are doped into g-C_3N_4, they act as electron acceptors that can enhance the ability of g-C_3N_4 to capture photogenerated charge carriers. In addition, they can accelerate the separation and transfer of electron-hole pairs. Kamila Kočí et al. (2020) deposited platinum (Pt) nanoparticles on the C_3N_4 catalyst surface (Pt / C_3N_4). Due to the strong electronic acceptance of Pt nanoparticles, the photocatalytic quantum efficiency of Pt / C_3N_4 catalyst was improved significantly. Non-metal doping changes the electronic structure of g-C_3N_4 with electronegativity properties of non-metal elements (B, O, I, P, S, etc.). Hu et al. (2020) doped iodine (I) into the open framework of g-C_3N_4 (iodine-doped g-C_3N_4, CNIX). The characterization results showed that the response range of g-C_3N_4 to visible light was expanded and the efficiency of photogenerated charge separation was improved. Heterojunction construction refers to the combination of semiconductors with different energy band structures, which is conducive to the transfer and separation of electron-holes as well as the broadening of the light absorption range. Yang (2020a) obtained the ultra-thin 2D / 2D Ti_3C_2 / g-C_3N_4 photocatalyst by calcining the mixture of Ti_3C_2 particles and urea. The formation of heterojunction enabled a close interface contact between Ti_3C_2 and g-C_3N_4. The CO_2 photoreduction activity on g-C_3N_4 coupling with Ti_3C_2 was soaringly enhanced compared with pure g-C_3N_4.

The photocatalytic activities of catalyst materials are closely related to their morphology and structure (Wang et al., 2020b). To a certain extent, the physical and chemical properties are determined by the morphological structure and dimension of the catalyst, which further affect its photocatalytic activities. Therefore, controlling the morphology and structure could be an effective way to improve the performance of g-C_3N_4. Due to the layered structure of g-C_3N_4, two-dimensional (2D) g-C_3N_4 can be acquired from the bulk g-C_3N_4 by means of calcination, sonication, alkali exfoliation, etc. Zhou et al. (2020c) conducted heat treatment on g-C_3N_4 and obtained ultra-thin macro-mesoporous carbon nitride nanosheets (denoted as mMCNNS) (Figures 1a-1f). Bulk g-C_3N_4 can also be made into one-dimensional (1D) g-C_3N_4 materials (like nanotubes, nanowires, nanorods, and so on.) with different lengths and diameters through mesoporous molecular sieves, silica, and other templates. Zheng et al. (2014) synthesized g-C_3N_4 with helical rod-like morphology (named HR-CN) by using mesoporous silica as a sacrificial template (shown in Figure 1g).

Compared with 1D / 2D g-C_3N_4, the three-dimensional g-C_3N_4 based materials (3D CNBMs) have a larger specific surface area and higher porosity. 3D CNBMs with a three-dimensional (3D) network have many superiorities in the catalytic applications. The huge specific surface area can greatly increase the number of active sites for adsorption and degradation of pollutants. Sunlight can form multiple reflections in the 3D framework to enhance the light absorption efficiency (Liu et al., 2021; Wang et al., 2021b). The 3D structure can efficiently prevent the agglomeration of catalysts and improve the stability of catalysts. It can improve the porosity, provide a porous channel for the transmission of electrons, and greatly improve the catalytic activities (Zhang et al., 2021; Zhao et al., 2021). The catalyst fixed in a 3D framework is easy for recycling. According to Figure 2, there has been a great increase in the number of publications and citations of 3D CNBMs since 2009.

This review accentuates an overview of the recent development and progress of 3D CNBMs. Other reviews on 3D g-C_3N_4 classified and summarized the synthesis methods from the perspective of synthesis pathways (Li et al., 2019). In this work, the synthesis methods are systematically discussed from the aspect of 3D g-C_3N_4 and 3D CNBMs respectively. This review not only discusses the application of 3D CNBMs as photocatalytic materials but also introduces the applications in photo-electro-

chemistry and electrochemistry as supplementary. Finally, possible improvements and perspectives of 3D CNBMs are proposed.

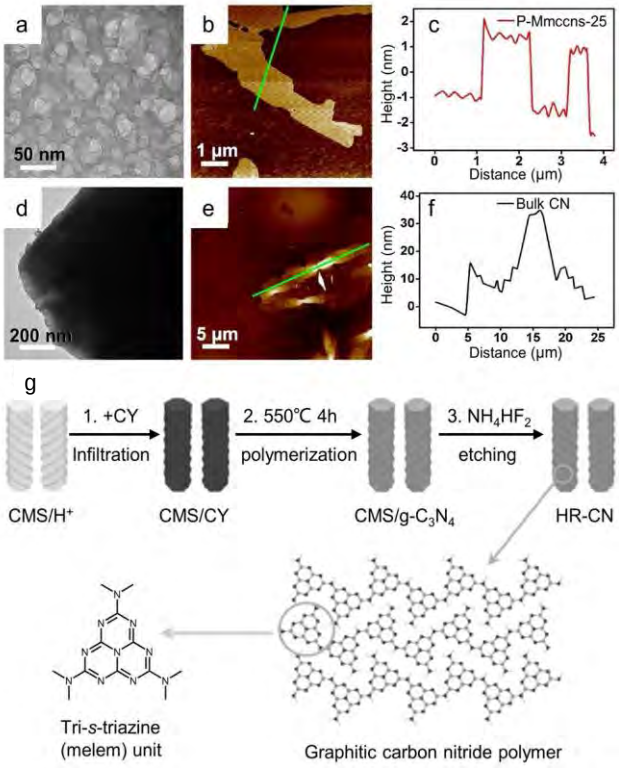

Figure 1. (a) (d) HRTEM image, (b) (e) AFM image and (c) (f) corresponding height image of P-mMCNNS-25 and bulk CN (Zhou et al., 2020c). Copyright © 2020 Elsevier. (g) Synthetic process of graphitic carbon nitride (Zheng et al., 2014). Copyright © 2014 WILEY-VCH Verlag GmbH & Co. KGaA, Weinheim.

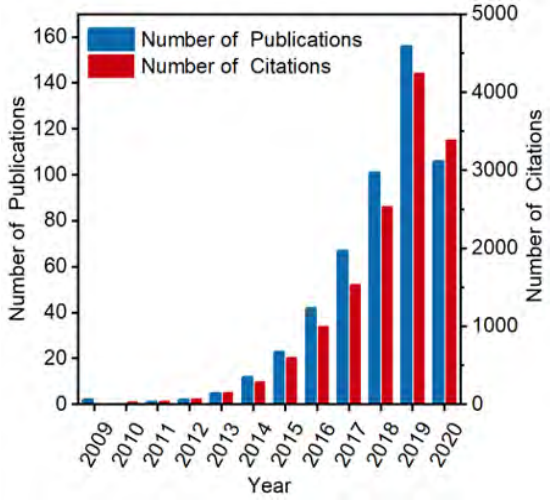

Figure 2. The annual collections of journal publications and citations concerning "graphitic carbon nitride" or "g-C_3N_4", and "3D" or "three-dimensional" subjects since 2009. Adapted from ISI Web of Science, dated 17th July 2020.

2. The Synthetic Method of Three-Dimensional Graphitic Carbon Nitride

The performance of the target materials is not only dependent on the precursors, but also largely contingent on the synthesis methods. This section creatively summarizes the synthesis methods from the perspective of three-dimensional carbon nitride materials, including hard template method, soft template method, and self-template method (Table 1).

2.1. Hard Template Method

Hard template method mostly uses rigid materials connected by covalent bonds as templates to regulate the morphology and size of materials. Chen et al. (2020) used SiO_2 spheres as templates, mixed it with melamine, and heated them in a covered crucible. In this process, melamine was mixed with SiO_2 to form g-C_3N_4@SiO_2 with a core-shell structure, and then the mixture was washed by a hydrofluoric acid solution to remove the silica template (Figure 3). In 2016, Tomer et al. (2016) used three-dimensional mesoporous SiO_2 as a hard template and designed a mesoporous Ag-loaded g-C_3N_4. The results showed that the 3D mesoporous structure generated a large number of active sites, and accelerated the transfer of charge carriers. With the load of appropriate amount of Ag nanoparticles, the photocurrent response was further increased to four times. Due to the high stability of hard templates, the size and morphology of nanomaterials can be controlled by this method, which can be used for mass production. Whereas toxic chemicals are needed to be removed from the templates in the end, as they can easily cause environmental pollution. Additionally, in the process of template removal, the pore structure may collapse, which can easily cause damage to the porous structure and affect the photocatalytic performance of the material (Xie et al., 2016).

2.2. Soft Template Method

Soft template method means that the free precursors are assembled regularly to form a collective with different spatial structures under the action of intermolecular force and spatial limitation ability. The common soft templates used to fabricate 3D CNBMs include microemulsion, biological molecule, bubble template, ionic liquid, etc (Mohamed et al., 2018; Zhang et al., 2018a; Qi et al., 2019; Tang et al., 2019; Zhao et al., 2020). Zhang et al. (2018) used oil emulsion droplets containing dissolved sulfur as a soft template to form materials with large pores. The templates were covered with GO-g-C_3N_4 sheets to assemble 3D porous sulfur/graphene@g-C_3N_4 (S/GCN). As the emulsion evaporated, the sulfur was uniformly "glued" to the walls of the g-C_3N_4 and wrapped inside at the same time. The microemulsion packaging method successfully obtained g-C_3N_4 cathode with sulfur content up to 82 wt% (Figure 4). Mohamed et al. (2018) designed and synthesized 3D porous microtubule carbon-doped g-C_3N_4 with kapok fiber (t-KF) as the biological molecule template by a simple thermal condensation method. T-KF served as both a biological template and an in-situ carbon dopant. The key to bubble templates is to form bubbles that prevent particles from sticking together. Tang et al. (2019) used ammonium

Table 1. The Synthetic Method of Three-Dimensional Graphitic Carbon Nitride

Methods	Pros	Cons	Template	Average Pore Sizes (nm)	BET Surface Area (m^2/g)	References
Hard template method	Easy to control size and morphology	Cause contamination	SiO_2	12.40	159.70	(Chen et al., 2020)
			mesoporous SiO_2	5.20	170.80	(Tomer et al., 2016)
Soft template method	Do not need to remove the template	Poor stability compared with hard template method	kapok fiber	27.80	49.60	(Mohamed et al., 2018)
			NH_3 and HCl gases	N/A	103.10	(Tang et al., 2019)
			ionic liquid	15.00	381.00	(Zhao et al., 2020)
			NaCl	N/A	33.60	(Ai et al., 2019)
Self-template method	Easy to operation, low cost, and low pollution	Not well known	cyanuric aci melamine d-supramolecular	20.00	130.00	(Chen et al., 2019)
			Melamine-cyanuric acid-urea supramolecular	18.19	42.15	(Gu et al., 2020)
			melamine-cyanuric acid supramolecular	N/A	58.50	(Zhou et al., 2019a)

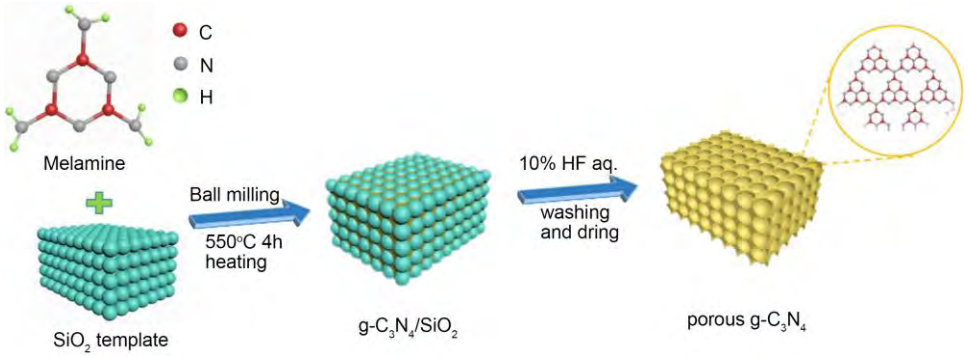

Figure 3. Schematic illustration of the 3D porous g-C_3N_4 fabrication procedures(Chen et al., 2020). Copyright © 2020 Elsevier.

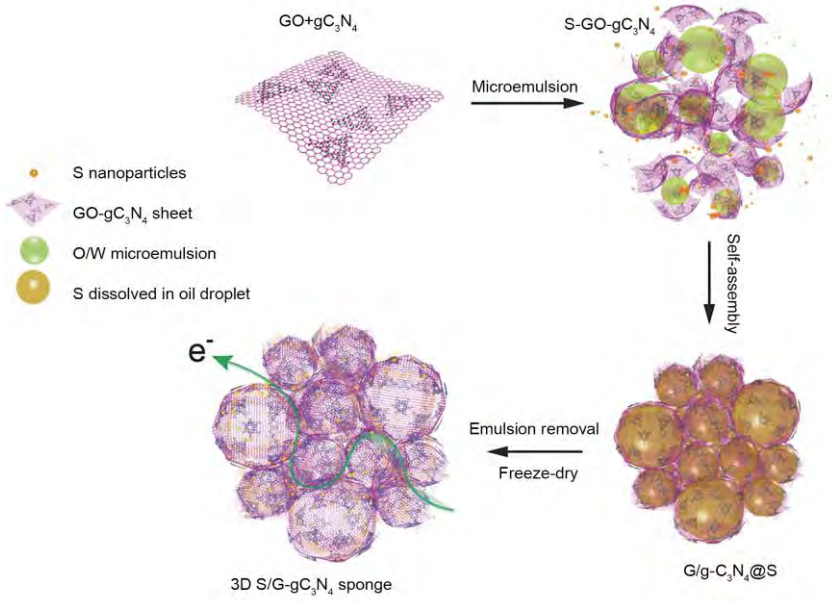

Figure 4. The procedure for preparing S/GCN hybrid sponge (Zhang et al., 2018a). Copyright © 2018 WILEY-VCH Verlag GmbH & Co. KGaA, Weinheim.

chloride (NH_4Cl) as a gas template to synthesize ultra-thin bubble-like g-C_3N_4 materials. In the synthetic process, NH_4Cl was decomposed into gaseous NH_3 and HCl after heating, and these gases aggregated on g-C_3N_4 to fabricate bubble modes. At the same time, the bubble molds expanded under the action of hot air, further preventing the inter-layer accumulation of g-C_3N_4. The self-assembly behavior of ionic liquids and the properties that they can form hydrogen bonds affect the structure of carbon nitride aggregates. Zhao et al. (2020) successfully prepared 3D mesoporous carbon nitride materials by decomposing ionic liquid (1-butyl-3-vinylimidazolium bromide) and precursor (cyanurate-melamine supramolecular aggregate) under high-temperature calcination. Compared with the conventional template method, the salt template directly adopts the soluble salt as the template which can effortlessly be removed by immersing in water. Ai et al. (2019) tuned the 3D porous structure of carbon nitride through sodium chloride (NaCl) templates. NaCl introduced metal ligands as donors and cyano groups as acceptors to participate in the construction of internal donor-acceptor (D-A) heterostructures, greatly promoting the separation of carriers. According to the experiment, the photocurrent density of MnO_x-decorated 3D porous C_3N_4 was nearly triple than that of bulk g-C_3N_4. Applying the soft template method does not need to remove the template. While materials synthesized by soft template method generally have poor stability compared with hard template method.

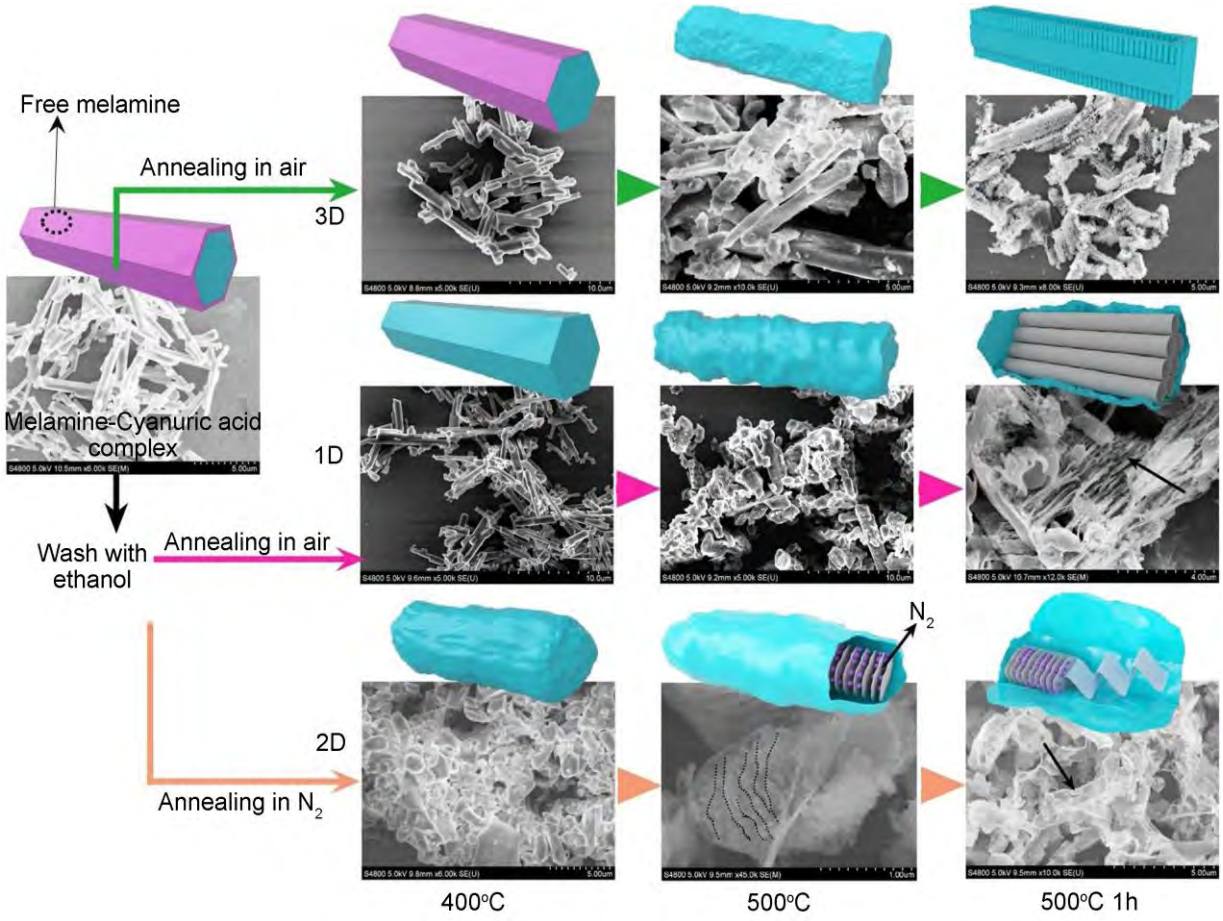

Figure 5. Fabrication process of g-C_3N_4 with different structure (Zhou et al., 2019a). Copyright © 2019 Elsevier.

2.3. Self-Template Method

Molecular self-assembly is a method to assemble monomers (such as melamine, cyanuric acid, barbiturate, or derivatives) into supramolecular aggregates by hydrogen bonds, Van Der Waals Forces, or electrostatic interaction for controlling structures (Tian et al., 2014; Zhang et al., 2015; Huo et al., 2018). This method has the characteristics of simple operation, low cost, and low pollution. Chen et al. (2019) synthesized 3D g-C_3N_4 by a simple self-template method. In this synthetic process, melamine and cyanuric acid were dissolved in water and then self-assembled to a 3D network of cyanurate-melamine supramolecular precursors. Then, a pale-yellow 3D g-C_3N_4 sample was produced by polycondensation at high temperatures. The 3D framework was assembled from highly crystalline ultrathin nanosheet units, providing a pathway for faster carrier transport. In addition, 3D g-C_3N_4 maintained stability for more than 100 h in the whole water decomposition reaction thanks to its 3D structure that prevented the agglomeration of nanomaterials. Gu et al. (2020)

synthesized 3D porous g-C_3N_4 by supramolecular self-assembly of melamine, cyanuric acid and urea under appropriate conditions, and used this material as a carrier to load ammonium vanadate (V-IL/3D g-C_3N_4) for aerobic oxidation and desulfurization by a thermal solvent method. Based on the characterization results, the BET surface area of ammonium vanadate (V-IL) was greatly increased as it was uniformly loaded on the 3D porous g-C_3N_4, thus exposing more active sites. By changing the heat treatment conditions, the geometric size and morphological structure of carbon nitride can be controlled. Zhou et al. (2019a) used melamine and cyanuric acid as precursors and set different heat treatment parameters. They successfully obtained graphitic carbon nitride with a 3D towel gourd structure, a 2D nanosheet structure, and a 1D nanotube structure, respectively (Figure 5).

Table 2. The Synthetic Method of Three-Dimensional Graphitic Carbon Nitride Based Materials

Methods		Prons	Cons	Catalyst	Average pore Sizes (nm)	BET surface area (m^2/g)	References
In-situ grown	Thermal polymerization	Wide applicability	High energy consumption	g-C_3N_4/MgO	14.44	83.37	(Zhou et al., 2018)
				g-C_3N_4/NiO	N/A	123.60	(Wang et al., 2019a)
				WC_{1-x}/g-C_3N_4	N/A	99.70	(Xiong et al., 2019)
	Freeze-drying	Good control over morphology and high structure stability	Not well known	g-C_3N_4/cellulose	N/A	128.97	(Bai et al., 2020)
	Heat-cooling	Easy to operation	Not well known	g-C_3N_4-agar	N/A	38.04	(Tan et al., 2019)
Hydrothermal/solvent-thermal		Mild reaction conditions and less hard agglomeration	Depend on the reaction equipment and produce waste liquid	g-C_3N_4/SnS_2	N/A	51.40	(Sun et al., 2014)
				g-C_3N_4/α-Fe_2O_3	N/A	119.60	(Kim et al., 2020)
				CdS/ g-C_3N_4	N/A	22.23	(Liu et al., 2020)

3. The Synthetic Method of Three-Dimensional Graphitic Carbon Nitride Based Materials

By adding other components in the process of material synthesis can overcome the poor performance of single-component photocatalysts. This section summarizes the synthesis methods of 3D graphitic carbon nitride based composite materials, which are mainly divided into thermal polymerization, freeze-drying, heat-cooling, hydrothermal / solvent-thermal, etc (Table 2).

3.1. In-Situ Grown

3.1.1. Thermal Polymerization

Thermal polymerization is a method in which molecular monomers condensate into graphitic carbon nitride polymers under thermal calcination (Zhou et al., 2020b). Because of the small specific surface area, pure graphitic carbon nitride is often modified with other materials to produce 3D CNBMs composites. Zhou et al. (2018) simply calcined the mixed solution of melamine and $MgCl_2$ to obtain a three-dimensional g-C_3N_4 / MgO composite photocatalyst. It has abundant adsorption sites, a three-dimensional network structure, and a rough surface morphology. Wang et al. (2019a) prepared spherical flower-shaped g-C_3N_4 / NiO heterojunction composites by calcination and hy-drothermal methods. In the synthetic process, g-C_3N_4 was obtained through the first calcination, and then the obtained g-C_3N_4 was mixed with nickel nitrate and urea, and transferred to the sealed high-pressure reactor for 12 hours. The three-dimensional spherical flower g-C_3N_4 / NiO composite photocatalysts were obtained after the second calcination. G-C_3N_4 was composed of smooth flat nanosheets with a layered structure, while pure NiO had a spherical structure. After the hydrothermal reaction, the different nanosheets were assembled and combined with NiO, resulting in the formation of coarse and dense "petals" (g-C_3N_4) on the NiO surface. Three-dimensional flower-shaped g-C_3N_4/NiO exhibited a larger BET surface area than pure g-C_3N_4 and pure NiO, which were 2.06 and 2.12 times respect-tively. Xiong et al. (2019) firstly synthesized hexacarbonyl tungsten / melamine composite precursors with $W(CO)_6$ and melamine as the initial reactants by sonochemical method. Then, the final product of g-C_3N_4 / WC_{1-x} was obtained after calcination step by step (shown in Figure 6). The first 8 h calcination in Ar / H_2 mixed atmosphere was to promote the pyrolysis of tungsten-based compounds and the condensation of melamine. The second step was to induce the formation of nitrogen defects to form g-C_3N_x / WC_{1-x} (g-C_3N_4 for nitrogen defects is labeled g-C_3N_x). In the whole pyrolysis process, 2D WC_{1-x} / g-C_3N_4 nanosheet was spontaneously combined into a three-dimensional structure.

3.1.2. Freeze-Drying

Freeze-drying is mainly used to obtain the aerogels with 3D porous structure. In this process, water goes through two-phase transitions. First, water solidifies from liquid water into solid water (i.e., ice crystal), and then the solid water sublimates into gaseous water. Loose and porous materials can be obtained by this method as the water is directly sublimated from the ice crystals into the gaseous phase and escapes out. The dried materials replicate the ice crystal structure without condensation and collapse, which can effectively avoid the destruction of the original structure morphology. Wan et al. (2016) obtained the C_3N_4/ graphene oxide macroscopic aerogel (C_3N_4 / GOA) composites

Transmission Electron Microscope (TEM) images. Tan et al. (2019) used agar and g-C_3N_4 powder as raw materials to obtain g-C_3N_4-agar hybrid aerogel through the heat-cooling polymerization process. The g-C_3N_4-agar mixture aerogels showed improved light absorption and photocurrent response capability. Moreover, the 3D network structure not only showed excellent adsorption performance but also could overcome the difficulty in recycling the powder catalyst.

3.2. Hydrothermal / Solvent-Thermal

Hydrothermal / solvent-thermal refers to the preparation of composite materials by placing the precursor in water / solvent under high temperature and pressure. Sun et al. (2014) synthesized 3D flower-shaped g-C_3N_4 / SnS_2 composites by hydrothermal method. This composites with heterojunction structure presented wider light absorption and faster photocurrent responses. Kim et al. (2020) prepared g-C_3N_4 / α-Fe_2O_3 / graphene aerogels (CNFGA) by using graphene oxide (GO), g-C_3N_4, and $FeCl_3$ as raw materials through a simple hydrothermal method (shown in Figure 9). $FeCl_3$ hydrolyzed and interacted with the oxygen groups on GO board via static electricity, forming FeOOH deposition on 2D GO. Then the mixture combined with g-C_3N_4 nanosheets in an autoclave. In the process of hydrothermal, GO changed into reduced graphene oxide (rGO) and FeOOH changed into α-Fe_2O_3. Liu et al. (2020) calcined melamine at 550 °C to obtain yellow powder g-C_3N_4, and then g-C_3N_4 was added into isopropyl alcohol solution for sonication for 6 h. The CdS / g-C_3N_4 composites were then synthesized through solvent-thermal reaction by using cadmium sulfate and thiourea as cadmium sources and sulfur sources respectively. This material not only had a 2D / 2D close contact interface but also had a 3D layered framework. The hydrothermal / solvent-thermal method is mild, which can avoid hard agglomeration in the calcination process. However, the reaction conditions of high temperature and high pressure make it depend on the reaction equipment. In addition, it is necessary to solve the problem of waste liquid caused by hydrothermall / solvent-thermal method.

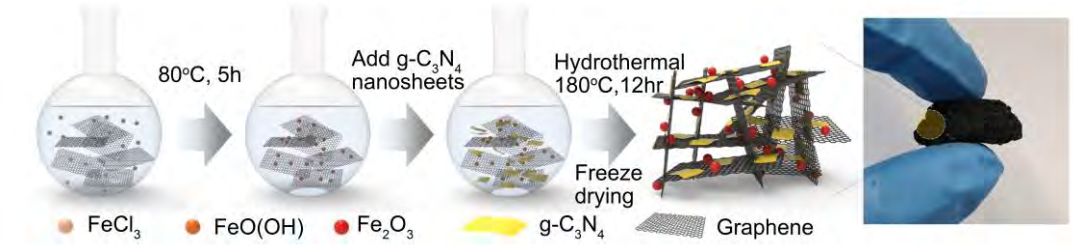

Figure 9. The synthesis procedure of CNFGA (Kim et al., 2020). Copyright © 2020, John Wiley and Sons.

4. The Application of Three-Dimensional Graphitic Carbon Nitride Based Materials

4.1. Photocatalytic Applications

3D CNBMs have received enormous attention for water splitting, organic pollutants degradation, and CO_2 reduction in solar photocatalysis due to the large specific area, plentiful active sites, and excellent electrical conductivity. The detailed applications in photocatalysis are as follows.

4.1.1. Organic Pollutants Degradation

3D CNBMs photocatalysts have been widely used in the degradation and mineralization of organic pollutants, mainly including dyes, antibiotics, pesticides, and so on (Yuan et al., 2016; Sheng et al., 2019; Wang et al., 2019b; Gupta et al., 2020; Si et al., 2020; Yang et al., 2020c;). The electrons in the valence band can be excited to the conduction band under the irradiation of solar energy, generating oxidative holes and reductive electrons to mineralize organic pollutants. The 3D structure of CNBMs can provide multi-dimensional transport channels, effectively promoting the separation and transfer of photo-generated electron-hole pairs, thereby greatly improving the photocatalytic performance.

In 2015, Zhang et al. (2015) applied 3D CNBMs in organic pollutants degradation for the first time. They hybridized graphene / g-C_3N_4 and Ag@$AgVO_3$ nanowires for the removal of methylene blue, promoting the possibility of the applications of 3D composites in environmental protection. After that, Li et al. (2018b) synthesized a highly efficient g-C_3N_4 / TiO_2 / kaolinite composite, which exhibited high degradation ability to ciprofloxacin (CIP) and high disinfection ability towards *S. aureus*. The superoxide radical ($\cdot O_2^-$) was proved to be the main active species in the procedure of CIP removal. Liu et al. (2019) discussed the influences of other antibiotics and water sources in evaluating photocatalytic performance of g-C_3N_4 / Ag_2CO_3 / graphene oxide (CN / AC / GO) composite to degrade tetracycline (TC). The composite material showed highly efficiency to the degradation of OTC-HCL and LVFX. The degradation rates of TC by CN / AC / GO in actual wastewater samples only slightly decreased, which indicated a good application potential in environmental remediation. Gupta et al. (2020) prepared atom-thin sulfur-doped g-C_3N_4 / ZnO photocatalysts. This interconnected 3D porous structure consisted of 2D graphitic thin plates and ZnO nanoscale plates. Its degradation rate of CIP was up to 98%, which was 18 and 38% higher than that of ZnO and s-g-C_3N_4, respecttively. Table S1 shows the applications of 3D CNBMs for degrading organic pollutants.

4.1.2. Water Splitting for Hydrogen Production

Hydrogen is recognized as a clean energy source in the world.

In the absence of sacrificial agents, using solar energy as the driving force to split water into hydrogen and convert solar energy to hydrogen energy can effectively reduce human dependence on non-renewable energy sources such as fossil fuels and alleviate the energy crisis (Yan et al., 2011; Lu et al., 2014; Zhou et al., 2015; Fu et al., 2019). The core of semiconductor photocatalyst for photocatalytic total water splitting under the action of visible light lies in the bandgap of the catalyst and the position of the valence band and conduction band. Specifically, the top of the valence band must be more positive than the O_2 / H_2O redox potential, and the bottom of the conduction band must be more negative than the H^+ / H_2 0 V (vs. NHE) redox potential (Kudo et al., 2009). In theory, g-C_3N_4 has the innate advantage of total water splitting. However, oxygen production is a complex four-electron reaction, so the photolysis of water is still dominated by hydrogen production (Liu et al., 2012).

Shen et al. (2014) synthesized a novel porous g-C_3N_4 with high performance of visible-light photocatalytic H_2 evolution by using cyanuric acid. In their experiment, cyanuric acid was used as a polymerization inhibitor due to the strong hydrogen bond with melamine. Luo et al. (2018) proposed a simple method to generate 3D spongy g-C_3N_4 via a combination treatment of acid protonation and thermal oxidation to bulk g-C_3N_4. Experimental results showed that these two treatments had a positive effect on the rate of hydrogen evolution. Qian et al. (2019) successfully synthesized 3D porous g-C_3N_4. The porous structure had many advantages, such as large specific surface area, highly efficient charge separation and fast electron transfer efficiency. Owing to this unique structure, the rate of hydrogen evolution catalyzed by porous g-C_3N_4 was up to 598 $mol \cdot h^{-1} \cdot g^{-1}$ and the apparent quantum yield at 420 nm was 3.31%. Zhou et al. (2020a) successfully synthesized thin-shell honeycomb g-C_3N_4 (g-C_3N_4-TSH) with melamine and NH_4Cl for photocatalytic hydrogen evolution. It has been certificated that the photoelectron migration distance had been diminished which boosted the mass transfer owing to its special thin-shell honeycomb structure. The apparent quantum efficiency was 9.86%, which was better than many reported modified g-C_3N_4. Table S2 shows the 3D CNBMs for H_2 production.

4.1.3. CO_2 Reduction

Due to the over-reliance on fossil fuels in the modern industry, the emission of CO_2 is serious. The use of solar energy to convert CO_2 into green fuel is an environmentally friendly and energy-saving approach to deal with the global energy crisis and greenhouse effect. The process of CO_2 conversion is the reaction of CO_2 reduction by electrons (He et al., 2015; Wang et al., 2015b; Ye et al., 2015; Di et al., 2017; Fu et al., 2017).

Wang et al. (2018b) utilized 3D g-C_3N_4 / C composites as photocatalysts for the reduction of CO_2. Photocatalytic measurements indicated that these composites showed higher activity for CO_2 reduction with CO and CH_4 yield of 229 and 112 $\mu mol \cdot g^{-1}$. It is obvious that the improvement of photocatalytic performance was mainly because of the modification of its structure and the enhancement of light capture and better CO_2 adsorption capacity. Wang et al. (2018b) synthesized a new g-C_3N_4 / $BiFeWO_x$ heterojunction photocatalyst by in-situ solvent-thermal method. In this way, a tight chemical bond interface can be established between $BiFeWO_x$ and g-C_3N_4. Due to the interface interaction, g-C_3N_4 / $BiFeWO_x$ heterojunction catalysts showed high visible light sensitivity and efficient carrier separation and transfer. Under visible light irradiation, the yield of CO production by CO_2 reduction (43 $mol \cdot h^{-1} \cdot g^{-1}$) was higher than that of pure $BiFeWO_x$ (5.2 $mol \cdot h^{-1} \cdot g^{-1}$) and g-$C_3N_4$ (8.9 $mol \cdot h^{-1} \cdot g^{-1}$). Recently, Sun et al. (2020a) used template method and microwave method to load copper nanoparticles (Cu-NPS) on the special g-C_3N_4 foam to obtain Cu / CF composite materials. On the one hand, the 3D porous structure of foam-shaped semicon-ductor photocatalyst provided gas transmission channel for CO_2 absorption and diffusion. On the other hand, 0D metal nanoparticles loaded on 3D semi-conductors formed a heterojunction, which inhibited the recombination of electron and hole and promoted photogenerated charge separation efficiency. Table S3 shows the applications of 3D CNBMs for CO_2 reduction.

4.2. Photo-Electrochemical Applications

3D CNBMs, as excellent photosensitive materials, have the characteristics of strong light capture ability and high charge separation rate, which can be used in the photoelectrochemical analysis. Wen et al. (2020) synthesized cathode materials based on the synthesized three-dimensional ZnO / Au / g-C_3N_4 heterojunction composites for photochemical water decomposition. The photocathode of ZnO / Au / g-C_3N_4 loaded with platinum co-catalyst showed excellent hydrogen production rate and Faraday efficiency in the experiment. 3D CNBMs not only can be directly used in the fabrication of photocathodes but also can be the promising candidate in photoelectro-chemical sensors. Du and co-authors prepared a simple PEC sensor based on 3D branched crystalline carbon nitride (3D BC-C_3N_4) to detect traces of Cu^{2+} in water (Du et al., 2020). The lowest detection concentration reached 0.38 nM, which was comparable to or even better than previously reported studies. Lv et al. (2020) synthesized F8BT / g-C_3N_4 heterojunction with organic polymer semiconductor and used it as photosensitive material and constructed a sensitive PEC sensor for carcinoembryonic antigen (CEA) detection. The sensor showed good performance, such as satisfactory selectivity, acceptable accuracy, and high sensitivity, indicating the potential in cancer biomarkers.

4.3. Electrochemical Applications

Oxygen reduction reaction (ORR) is the pivotal reaction in energy storage devices. At present, Platinum-based materials are the most efficient electrocatalysts in ORR. Hoverer, the expensive cost and limited availability have restricted the development (Gu et al., 2016; Wang et al., 2018c). 3D CNBMs are cheap materials with good physicochemical stability. They have a high content of nitrogen elements, which can be the potential sites to modify the electronic structures and the electroconductivity properties (Liu and Zhang, 2013; Tian et al., 2014). 3D CNBMs would be the potential materials to replace Pt-based electrocatalysts. Specifically, they can be used as ORR electrocatalyst in polymer electrolyte membrane fuel cell (PEMFC). Qin et al. (2014) designed and prepared mesoporous carbon nitride/graphene composites and used them as an electrocatalyst for ORR in PEMFC.

As a consequence of the hollow and mesoporous structure, this electrocatalyst showed remarkably strengthened electrocatalytic activity and excellent resistance in methanol, indicating a promising application prospect in PEMFC. Also, the 3D CNBMs bifunctional electrocatalysts with oxygen reduction / evolution reactions (ORR / OER) can be reasonably designed and prepared, which is particularly important for promoting the development of metal-air battery. Wu et al. (2017) designed and prepared ultrathin N-doped carbon / g-C_3N_4 composites. The unique loofa-like 3D network structure of the material showed obvious ORR activity and excellent OER activity, which had great application potential in the production of bifunctional catalysts. Li and co-authors prepared cobalt catalyzed nitrogen-doped carbon nanotubes based on g-C_3N_4 materials and applied this catalyst into self-made zinc-air batteries (Li et al., 2018c). This battery showed high specific capacity and excellent cycling stability. Additionally, 3D CNBMs are low-cost materials with excellent electrical conductivity, which supports vertical charge transfer during charging and discharging, and they have potential applications in supercapacitors. Zhou and his colleges victoriously prepared 3D PCN@V_2O_5 electrodes (Zhou et al., 2020e). In the electrochemical performance test, the PCN@V_2O_5 electrode showed a high specific capacity with 457 Fg^{-1} at 0.5 Ag^{-1} and outstanding cycling performance which could perpetuate good performance after 500 cycles. Moreover, 3D CNBMs are considered to be promising candidate materials for electrochemical sensors by reason of the chemical stability, electrical conductivity, considerable specific surface area, and enormous active sites. Wang and co-authors prepared a glass carbon electrode based on multi-walled carbon nanotubes /g-C_3N_4 nanosheets (MWNTs / g-C_3N_4) (Wang et al., 2016a). This porous and loose structure made the g-C_3N_4 / MWNTs / GCE show high sensitivity to dopamine, uric acid, and tryptophan. What's more, the sensor had been successfully used to measure these compounds in human serum and urine samples.

5. Conclusions and Perspectives

In this review, the synthetic methods of 3D CNBMs and 3D CNBMs composites have been discussed in detail. The synthesis method of 3D CNBMs mainly includes hard template method, soft template method, and self-template method. Some methods like thermal polymerization, freeze-drying, heat-cooling, and hydrothermal / solvent-thermal have been also explored for synthesizing 3D CNBMs composites. Furthermore, 3D CNBMs have shown extensive applications in photocatalysis, electrochemistry, and photochemistry owing to their special electronic structure and band structure.

Compared with bulk g-C_3N_4, 3D CNBMs have more stable frameworks. However, there are still some problems and challenges needed to be considered:

(1) Although there are more and more studies on 3D CNBMs, most of them are based on the modification of 2D CNBMs. The 3D CNBMs are mostly obtained by means of doping modification and constructing heterogeneous composites. However, the modification studies based on 3D CNBMs are relatively few, and future research can be developed in this direction.

(2) Most studies on the performance of 3D CNBMs photocatalyst focus on the improvement of catalytic performance through modifications. However, there is a lack of research on the mechanism of how these modification methods can improve the catalytic activities.

(3) The porous structure of 3D CNBMs can effectively adsorb the reactant and provide the active sites, but the adsorption and desorption processes have been rarely studied. In future studies, it can be explored from the perspective of thermodynamics and kinetics.

(4) Despite the increasing studies on 3D CNBMs, there are relatively fewer reports on 3D CNBMs compared with g-C_3N_4. These studies mostly focus on applications in photocatalysis, and there are few studies in electrocatalysis and photo-electrocatalysis. Subsequent research can be conducted in diverse aspects to fully realize the value of 3D CNBMs.

Acknowledgements. This study was financially supported by the Program for the National Natural Science Foundation of China (U20A20323, 51879101), the National Program for Support of Top-Notch Young Professionals of China (2014), the Fundamental Research Funds for the Central Universities, Hunan Provincial Science and Technology Plan Project (No.2016RS3026, 2017SK2243, 2018SK20410), the Fundamental Research Funds for the Central Universities (531119200086, 531118010114, 531107050978, 541109060031, 531118010574), the Program for Changjiang Scholars and Innovative Research Team in University (IRT-13R17), and the Three Gorges Follow-up Research Project (2017HXXY-05).

References

Ai, M.H., Zhang, J.W., Gao, R.J., Pan, L., Zhang, X.W. and Zou, J.J. (2019). MnOx-decorated 3D porous C_3N_4 with internal donoracceptor motifs for efficient photocatalytic hydrogen production. *Appl. Catal. B*., 256, 117805. http://doi.org/10.1016/j.apcatb.2019.117805

Bai, W.D., Yang, X.Z., Du, X.L., Qian, Z.Q., Zhang, Y., Liu, L. and Yao, J.M. (2020). Robust and recyclable macroscopic g-C_3N_4/cellulose hybrid photocatalysts with enhanced visible light photocatalytic activity. *Appl. Surf. Sci*., 504, 144179. http://doi.org/10.1016/j.apsusc.2019.144179

Cao, J. and Zhou, Y. (2017). Excited state relaxation processes of H_2-evolving Ru-Pd supramolecular photocatalysts containing a linear or non-linear bridge: a DFT and TDDFT study. *Phys. Chem. Chem. Phys.,* 19(18), 11529-11539. http://doi.org/10.1039/c6cp07857e

Chen, W., Liu, M., Li, X.Y. and Mao, L.Q. (2020). Synthesis of 3D mesoporous g-C3N4 for efficient overall water splitting under a Z-scheme photocatalytic system. *Appl. Surf. Sci.*, 512, 145782. http://doi.org/10.1016/j.apsusc.2020.145782

Chen, X.J., Shi, R., Chen, Q., Zhang, Z.J., Jiang, W.J., Zhu, Y.F. and Zhang, T.R. (2019). Three-dimensional porous g-C_3N_4 for highly efficient photocatalytic overall water splitting. *Nano Energy*, 59, 644-650. http://doi.org/10.1016/j.nanoen.2019.03.010

Cheng, L., Xiang, Q.J., Liao, Y.L. and Zhang, H.W. (2018). CdS- Based photocatalysts. *Energy Environ. Sci*., 11(6), 1362-1391. http://doi.org/10.1039/c7ee03640j

Cheng, M., Liu, Y., Huang, D.L., Lai, C., Zeng, G.M., Huang, J.H., Liu, Z.F., Zhang, C., Zhou, C.Y. and Qin, L. (2019). Prussian blue analogue derived magnetic Cu-Fe oxide as a recyclable photo-Fenton catalyst for the efficient removal of sulfamethazine at near neutral pH values. *Chem. Eng. J*., 362, 865-876. http://doi.org/10.1016/j.cej.2019.01.101

Di Mauro, A., Fragalà, M.E., Privitera, V. and Impellizzeri, G. (2017). ZnO for application in photocatalysis: From thin films to nanostructures. *Mater. Sci. Semicond. Process*., 69, 44-51. http://doi.org/10.1016/j.mssp.2017.03.029

Di, T.M., Zhu, B.C., Cheng, B., Yu, J.G. and Xu, J.S. (2017). A direct Z-scheme g-C_3N_4/SnS_2 photocatalyst with superior visible-light CO_2 reduction performance. *J Catal*., 352, 532-541. http://doi.org/10.1016/j.jcat.2017.06.006

Dong, F., Zhao, Z.W., Xiong, T., Ni, Z.L., Zhang, W.D., Sun, Y.J. and Ho, W. (2013). In situ construction of g-C_3N_4/g-C_3N_4 metal-free heterojunction for enhanced visible-light photocatalysis. *ACS Appl. Mater. Interfaces*, 5(21), 11392-11401. http://doi.org/10.1021/am40 3653a

Du, J.Y., Fan, Y.F., Gan, X.R., Dang, X.M. and Zhao, H.M. (2020). Three-dimension branched crystalline carbon nitride: A high efficiency photoelectrochemical sensor of trace Cu^{2+} detection. *Electrochim*., 330, 135336. http://doi.org/10.1016/j.electacta.2019.135336

Duan, M., Jiang, L., Zeng, G., Wang, D., Tang, W., Liang, J., Wang, H., He, D., Liu, Z. and Tang, L. (2020). Bimetallic nanoparticles/metal-organic frameworks: Synthesis, applications and challenges. *Appl. Mater. Today*., 19, 100564. http://doi.org/10.1016/j.apmt.2020.100564

Fu, J.W., Xu, Q.L., Low, J.X., Jiang, C.J. and Yu, J.G. (2019). Ultrathin 2D/2D WO_3/g-C_3N_4 step-scheme H_2-production photocatalyst. *Appl. Catal. B*., 243, 556-565. http://doi.org/10.1016/j.apcatb.2018.11.011.

Fu, J.W., Zhu, B.C., Jiang, C.J., Cheng, B., You, W. and Yu, J.G. (2017). Hierarchical Porous O-Doped g-C_3N_4 with Enhanced Photocatalytic CO_2 Reduction Activity. *Small*, 13(15), 1603938. http://doi.org/10.1002/smll.201603938

Ge, M., Li, Y.F., Liu, L., Zhou, Z. and Chen, W. (2011). Bi_2O_3- Bi_2WO_6 Composite Microspheres: Hydrothermal Synthesis and Photocatalytic Performances. *J. Phys. Chem. C*., 115(13), 5220-5225. http://doi.org/10.1021/jp108414e

Golestanbagh, M., Parvini, M. and Pendashteh, A. (2018). Preparation, Characterization and Photocatalytic Properties of Visible-Light-Driven CuO/SnO_2/TiO_2 Photocatalyst. *Catal. Letters*, 148(7), 2162-2178. http://doi.org/10.1007/s10562-018-2385-5

Gu, J.Y., Liu, M.G., Xun, S.H., He, M.Q., Wu, L.L., Zhu, L.H., Wu, X.Y., Zhu, W.S. and Li, H.M. (2020). Lipophilic decavanadate supported by three-dimensional porous carbon nitride catalyst for aerobic oxidative desulfurization. *Mol. Catal.*, 483, 110709. http://doi.org/10.1016/j.mcat.2019.110709

Gu, W.L., Hu, L.Y., Li, J. and Wang, E. (2016). Hybrid of g-C_3N_4 Assisted Metal-Organic Frameworks and Their Derived High-Efficiency Oxygen Reduction Electrocatalyst in the Whole pH Range. *ACS Appl. Mater. Interfaces*, 8(51), 35281-35288. http://doi.org/10.1021/acsami.6b12031

Gupta, B., Gupta, A.K., Ghosal, P.S. and Tiwary, C.S. (2020). Photo-induced degradation of bio-toxic Ciprofloxacin using the porous 3D hybrid architecture of an atomically thin sulfur-doped g-C_3N_4/ ZnO nanosheet. *Environ. Res*., 183, 109154. http://doi.org/10.1016/j.envres.2020.109154

He, B., Liu, R., Ren, J.B., Tang, C.J., Zhong, Y.J. and Hu, Y. (2017). One-Step Solvothermal Synthesis of Petalous Carbon-Coated Cu^+-Doped CdS Nanocomposites with Enhanced Photocatalytic Hydrogen Production. *Langmuir,* 33(27), 6719-6726. http://doi.org/10.1021/acs.langmuir.7b01450

He, L., Li, Y.P., Zhu, F.P., Sun, X.M., Herrmann, H., Schaefer, T., Zhang, Q.Z. and Wang, S.G. (2020). Insight into the Mechanism of the OH-Induced Reaction of Ketoprofen: A Combined DFT Simulation and Experimental Study. *J. Environ. Inform*., 35(2), 128-137. http://doi.org/10.3808/jei.201900408

He, R.A., Zhou, J.Q., Fu, H.Q., Zhang, S.Y. and Jiang, C.J. (2018). Room-temperature in situ fabrication of Bi_2O_3/g-C_3N_4 direct Z-scheme photocatalyst with enhanced photocatalytic activity. *Appl. Surf. Sci.*, 430, 273-282. http://doi.org/10.1016/j.apsusc.2017.07.191

He, Y.M., Zhang, L.H., Teng, B.T. and Fan, M.H. (2015). New Application of Z-Scheme Ag_3PO_4/g-C_3N_4 Composite in Converting CO_2 to Fuel. *Environ. Sci. Technol*., 49(1), 649-656. http://doi.org/10.1021/es5046309

Hu, X.L., Zhang, W.J., Yong, Y.W., Xu, Y., Wang, X.H. and Yao, X.X. (2020). One-step synthesis of iodine-doped g-C_3N_4 with enhanced photocatalytic nitrogen fixation performance. *Appl. Surf. Sci*., 510, 145413. http://doi.org/10.1016/j.apsusc.2020.145413

Huang, G.W., Liu, H., Li, X. and Ma, M. (2019). Exploring Drivers of Nitrate Contamination of Drinking Water in an Arid Region of China. *J. Environ. Inform*., 33(2), 105-112. http://doi.org/10.3808/jei.201900409

Huang, J., Huang, G., An, C., Xin, X., Chen, X., Zhao, Y., Feng, R. and Xiong, W. (2020a). Exploring the use of ceramic disk filter coated with Ag/ZnO nanocomposites as an innovative approach for removing Escherichia coli from household drinking water. *Chemosphere,* 245, 125545. http://doi.org/10.1016/j.chemosphere. 2019.125545

Huang, Z.Z., Zeng, Z.T., Song, Z.X., Chen, A.W., Zeng, G.M., Xiao, R., He, K., Yuan, L., Li, H. and Chen, G.Q. (2020b). Antimicrobial efficacy and mechanisms of silver nanoparticles against Phanerochaete chrysosporium in the presence of common electrolytes and humic acid. *J. Hazard. Mater*., 383, 121153. https://doi.org/10.1016/j.jhazmat.2019.121153

Huo, R., Yang, X.L., Yang, J.Y., Yang, S.Y. and Xu, Y.H. (2018). Self-assembly synthesis of $BiVO_4$/Polydopamine/g-C_3N_4 with enhanced visible light photocatalytic performance. *Mater. Res. Bull.*, 98, 225-230. http://doi.org/10.1016/j.materresbull.2017.10.016

Ji, L., Huang, G.H., Niu, D.X., Cai, Y.P. and Yin, J.G. (2020). A Stochastic Optimization Model for Carbon-Emission Reduction Investment and Sustainable Energy Planning under Cost-Risk Control. *J. Environ. Inform*., 36(2), 107-118. http://doi.org/10.3808 /jei.202000428

Jiang, Z., Yang, F., Yang, G.D., Kong, L., Jones, M.O., Xiao, T. and Edwards, P.P. (2010). The hydrothermal synthesis of BiOBr flakes for visible-light-responsive photocatalytic degradation of methyl orange. *J. Photochem. Photobiol. A*., 212(1), 8-13. http://doi.org/10.1016/j.jphotochem.2010.03.004

Khan, A., Alam, U., Raza, W., Bahnemann, D. and Muneer, M. (2018). One-pot, self-assembled hydrothermal synthesis of 3D flower-like CuS/g-C_3N_4 composite with enhanced photocatalytic activity under visible-light irradiation. *J. Phys. Chem. Solids*, 115, 59-68. http://doi.org/10.1016/j.jpcs.2017.10.032

Kim, C., Cho, K.M., Park, K., Kim, K.H., Gereige, I. and Jung, H. (2020). Ternary Hybrid Aerogels of g-C_3N_4/α-Fe_2O_3 on a 3D Graphene Network: An Efficient and Recyclable Z-Scheme Photocatalyst. *ChemPlusChem*. 85(1), 169-175. http://doi.org/10.1002/cplu.201900688

Koci, K., Van, H.D., Edelmannova, M., Reli, M. and Wu, J.C.S. (2020). Photocatalytic reduction of CO_2 using Pt/C_3N_4 photocatalyts. *Appl. Surf. Sci.*, 503, 144426. http://doi.org/10.1016/j.apsusc.2019.144426

Kudo, A. and Miseki, Y. (2009). Heterogeneous photocatalyst materials for water splitting. *Chem. Soc. Rev*., 38(1), 253-278. http://doi.org/10.1039/B800489G

Li, B.Y., Cao, Z.H., Wang, S.X., Wei, Q. and Shen, Z.R. (2018a). $BiVO_4$ quantum dot-decorated $BiPO_4$ nanorods 0D/1D heterojunction for enhanced visible-light-driven photocatalysis. *Dalton Trans.*, 47 (30), 10288-10298. http://doi.org/10.1039/c8dt02402b

Li, C.Q., Sun, Z.M., Zhang, W.Z., Yu, C.H. and Zheng, S.L. (2018b). Highly efficient g-C_3N_4/TiO_2/kaolinite composite with novel three-dimensional structure and enhanced visible light responding ability towards ciprofloxacin and S. aureus. *Appl. Catal. B.*, 220, 272-282. http://doi.org/10.1016/j.apcatb.2017.08.044

Li, X., Xiong, J., Gao, X.m., Huang, J.t., Feng, Z.j., Chen, Z. and Zhu, Y.f. (2019). Recent advances in 3D g-C_3N_4 composite photocatalysts for photocatalytic water splitting, degradation of pollutants and CO2 reduction. *J. Alloys Compd.*, 802, 196-209. http://doi.org/10.1016/j.jallcom.2019.06.185

Si, Y., Zhang, X.X., Liang, T.T., Xu, X., Qiu, L.F., Li, P. and Duo, S.W. (2020). Facile in-situ synthesis of 2D/3D g-C_3N_4/Cu_2O heterojunction for high-performance photocatalytic dye degradation. *Mater. Res. Express*, 7(1), 015524. http://doi.org/10.1088/2053-1591/ ab6893

Silva, C.u.G., Jua´rez, R., Marino, T., Molinari, R. and Garcı´a, H. (2011). Influence of Excitation Wavelength (UV or Visible Light) on the photocatalytic activity of titania containing gold nanoparticles for the generation of hydrogen or oxygen from water. *J. Am. Chem. Soc.*, 133(3), 595-602. http://doi.org/10.1021/ ja1086358

Sun, M., Yan, Q., Yan, T., Li, M.M., Wei, D., Wang, Z.P., Wei, Q. and Du, B. (2014). Facile fabrication of 3D flower-like heterostructured g-C_3N_4/SnS_2 composite with efficient photocatalytic activity under visible light. *Rsc Adv.,* 4(59), 31019-31027. http://doi.org/10.1039/c4ra03843f

Sun, Z.M., Fang, W., Zhao, L. and Wang, H.L. (2020). 3D porous Cu-NPs/g-C_3N_4 foam with excellent CO_2 adsorption and Schottky junction effect for photocatalytic CO_2 reduction. *Appl. Surf. Sci.*, 504, 144347. http://doi.org/10.1016/j.apsusc.2019.144347

Tan, L., Yu, C.F., Wang, M., Zhang, S.Y., Sun, J.Y., Dong, S.Y. and Sun, J.H. (2019). Synergistic effect of adsorption and photo- catalysis of 3D g-C_3N_4-agar hybrid aerogels. *Appl. Surf. Sci.*, 467-468, 286-292. http://doi.org/10.1016/j.apsusc.2018.10.067

Tang, J.Y., Kong, X.Y., Ng, B.J., Chew, Y.H., Mohamed, A.R. and Chai, S.P. (2019). Midgap-state-mediated two-step photoexcitation in nitrogen defect-modified g-C_3N_4 atomic layers for superior photocatalytic CO_2 reduction. *Catal. Sci. Technol*., 9(9), 2335-2343. http://doi.org/10.1039/c9cy00449a

Tian, J.Q., Ning, R., Liu, Q., Asiri, A.M., Alyoubi, A.O. and Sun, X.P. (2014). Three-Dimensional Porous Supramolecular Architecture from Ultrathin g-C_3N_4 Nanosheets and Reduced Graphene Oxide: Solution Self-Assembly Construction and Application as a Highly Efficient Metal-Free Electrocatalyst for Oxygen Reduction Reaction. *ACS Appl. Mater. Interfaces*, 6(2), 1011-1017. http://doi.org/10.1021/am404536w

Tomer, V.K., Thangaraj, N., Gahlot, S. and Kailasam, K. (2016). Cubic mesoporous Ag@CN: a high performance humidity sensor. *Nanoscale.* 8(47), 19794-19803. http://doi.org/10.1039/c6nr08039a

Wan, W.C., Yu, S., Dong, F., Zhang, Q. and Zhou, Y. (2016). Efficient C_3N_4/graphene oxide macroscopic aerogel visible-light photocatalyst. *J. Mater. Chem. A.* 4(20), 7823-7829. http://doi.org/10.1039/c6ta01804a

Wang, C., Li, J., Luo, X.Y., Hui, J.M., Liu, X., Tan, J. and Zhao, X. (2016a). Graphitic carbon nitride nanosheets modified multi-walled carbon nanotubes as 3D high efficient sensor for simultaneous determination of dopamine, uric acid and tryptophan. *J. Electroanal. Chem.*, 780, 147-152. http://doi.org/10.1016/j.jelechem. 2016.09.004

Wang, D.D., Li, J., Xu, Z.F., Zhu, Y.R., Chen, G.X. and Cui, Z. (2019a). Synthesis of g-C_3N_4/NiO p-n heterojunction materials with ball-flower morphology and enhanced photocatalytic performance for the removal of tetracycline and Cr^{6+}. *J. Mater. Sci*., 54(17), 11417-11434. http://doi.org/10.1007/s10853-019-03692-5

Wang, H., Wang, H.Q., Wang, Z.W., Tang, L., Zeng, G.M., Xu, P., Chen, M., Xiong, T., Zhou, C.Y., Li, X.Y., Huang, D.L., Zhu, Y., Wang, Z.X. and Tang, J.W. (2020a). Covalent organic framework photocatalysts: structures and applications. *Chem. Soc. Rev.*, 49 (12), 4135-4165. http://doi.org/10.1039/d0cs00278j

Wang, H.q., Zhang, X.D., Xie, J.F., Zhang, J.J., Ma, P., Pan, B.C. and Xie, Y. (2015a). Structural distortion in graphitic-C_3N_4 realizing an efficient photoreactivity. *Nanoscale.* 7(12), 5152-5156. http://doi.org/10.1039/c4nr07645a

Wang, J.X., Huang, J., Xie, H.L. and Qu, A.L. (2014). Synthesis of g-C_3N_4/TiO_2 with enhanced photocatalytic activity for H_2 evolution by a simple method. *Int. J. Hydrog. Energy*, 39(12), 6354-6363. http://doi.org/10.1016/j.ijhydene.2014.02.020

Wang, K., Li, Q., Liu, B.S., Cheng, B., Ho, W.K. and Yu, J.G. (2015b). Sulfur-doped g-C3N4 with enhanced photocatalytic CO_2- reduction performance. *Appl. Catal. B*, 176, 44-52. http://doi.org/10.1016/j.apcatb.2015.03.045

Wang, L., Liu, S., Wang, Z., Zhou, Y., Qin, Y. and Wang, Z.L. (2016b). Piezotronic Effect Enhanced Photocatalysis in Strained Anisotropic ZnO/TiO_2 Nanoplatelets via Thermal Stress. *ACS Nano*., 10(2), 2636-2643. http://doi.org/10.1021/acsnano.5b07678

Wang, W.J., Zeng, Z.T., Zeng, G.M., Zhang, C., Xiao, R., Zhou, C.Y., Xiong, W.P., Yang, Y., Lei, L. and Liu, Y. (2019b). Sulfur doped carbon quantum dots loaded hollow tubular g-C_3N_4 as novel photocatalyst for destruction of Escherichia coli and tetracycline degradation under visible light. *Chem. Eng. J*., 378, 122132. http://doi.org/10.1016/j.cej.2019.122132

Wang, W.J., Niu, Q.Y., Zeng, G.M., Zhang, C., Huang, D.L., Shao, B.B., Zhou, C.Y., Yang, Y., Liu, Y.X., Guo, H., Xiong, W.P., Lei, L., Liu, S.Y., Yi, H., Chen, S. and Tang, X. (2020b). 1D porous tubular g-C_3N_4 capture black phosphorus quantum dots as 1D/0D metal-free photocatalysts for oxytetracycline hydrochloride degradation and hexavalent chromium reduction. *Appl. Catal. B*, 273, 119051. http://doi.org/https://doi.org/10.1016/j.apcatb.2020.119051

Wang, W.J., Zhou, C.Y., Yang, Y., Zeng, G.M., Zhang, C., Zhou, Y., Yang, J.N., Huang, D.L., Wang, H., Xiong, W.P., Li, X.P., Fu, Y.K., Wang, Z.W., He, Q.Y., Jia, M.Y. and Luo, H.Z. (2021a). Carbon nitride based photocatalysts for solar photocatalytic disinfection, can we go further? *Chem. Eng. J.*, 404, 126540. http://doi.org/10.1016/j.cej.2020.126540

Wang, X., Li, Q., Gan, L., Ji, X., Chen, F., Peng, X. and Zhang, R. (2021b). 3D macropore carbon-vacancy g-C_3N_4 constructed using polymethylmethacrylate spheres for enhanced photocatalytic H_2 evolution and CO_2 reduction. *J. Energy Chem.*, 53, 139-146. http://doi.org/10.1016/j.jechem.2020.05.001

Wang, X., Maeda, K., Thomas, A., Takanabe, K., Xin, G., Carlsson, J.M., Domen, K. and Antonietti, M. (2009a). A metal-free polymeric photocatalyst for hydrogen production from water under visible light. *Nat. Mater*., 8(1), 76-80. http://doi.org/10.1038/nmat2317

Wang, X.C., Chen, X.F., Thomas, A., Fu, X.Z. and Antonietti, M. (2009b). Metal-containing carbon nitride compounds: a new functional organic-metal hybrid material. *Adv. Mater.*, 21(16), 1609-1612. http://doi.org/10.1002/adma.200802627

Wang, Y.G., Xia, Q.N., Bai, X., Ge, Z.G., Yang, Q., Yin, C.C., Kang, S.F., Dong, M.D. and Li, X. (2018a). Carbothermal activation synthesis of 3D porous g-C_3N_4/carbon nanosheets composite with superior performance for CO_2 photoreduction. *Appl. Catal. B*, 239, 196-203. http://doi.org/10.1016/j.apcatb.2018.08.018

Wang, Y.N., Zeng, Y.Q., Wan, S.P., Cai, W., Song, F.J., Zhang, S.L. and Zhong, Q. (2018b). In Situ Fabrication of 3D Octahedral g-C_3N_4/BiFeWO*x* Double-Heterojunction for Highly Selective CO_2 Photoreduction to CO Under Visible Light. *Chemcatchem*., 10(20), 4578-4585. http://doi.org/10.1002/cctc.201800959

Wang, Y.Q., Yin, X., Shen, H.B., Jiang, H., Yu, J.W., Zhang, Y.F., Li, D.W., Li, W.Z. and Li, J. (2018c). Co_3O_4@g-C_3N_4 supported on N-doped graphene as effective electrocatalyst for oxygen reduction reaction. *Int. J. Hydrog. Energy*., 43(45), 20687-20695. http://doi.org/10.1016/j.ijhydene.2018.09.140

Wang, Z.W., Wang, H., Zeng, Z.T., Zeng, G.M., Xu, P., Xiao, R., Huang, D.L., Chen, X.J., He, L.W. and Zhou, C.Y. (2020c). Metal-organic frameworks derived $Bi_2O_2CO_3$/porous carbon nitride: A nano-sized Z-scheme systems with enhanced photocatalytic activity. *Appl. Catal. B*, 267, 118700. http://doi.org/10.1016/j.apcatb.2020.118700

Wen, P., Sun, Y.H., Li, H., Liang, Z.Q., Wu, H.H., Zhang, J.C., Zeng, H.J., Geyer, S.M. and Jiang, L. (2020). A highly active three-dimensional Z-scheme ZnO/Au/g-C_3N_4 photocathode for efficient photoelectrochemical water splitting. *Appl. Catal. B*, 263, 118180. http://doi.org/10.1016/j.apcatb.2019.118180

Wu, H.P., Chen, J., Zeng, G.M., Xu, J.J., Sang, L.H., Liu, Q., Dai, J., Xiong, W.P., Yuan, Z., Wang, Y.Q. and Ye, S.J. (2020). Effects of Early Dry Season on Habitat Suitability for Migratory Birds in China's Two Largest Freshwater Lake Wetlands after the Impoundment of Three Gorges Dam. *J. Environ. Inform.*, 36(2), 82-92. http://

irradiation. *Rsc. Adv.*, 6(17), 14002-14008. http://doi.org/10.1039/c5ra22732a

Zhao, S., Huang, W.W., Wang, X.Q., Fan, Y.R. and An, C.J. (2019). Sorption of Phenanthrene onto Diatomite under the Influences of Solution Chemistry: A Study of Linear Sorption based on Maximal Information Coefficient. *J. Environ. Inform.*, 34(1), 35-44. http://doi.org/10.3808/jei.201600329

Zhao, S., Fang, J.S., Wang, Y.Y., Zhang, Y.W., Zhou, Y.M. and Zhuo, S.P. (2020). Construction of three-dimensional mesoporous carbon nitride with high surface area for efficient visible-light-driven hydrogen evolution. *J. Colloid Interface Sci.*, 561, 601-608. http://doi.org/10.1016/j.jcis.2019.11.035

Zhao, X., Guan, J., Li, J., Li, X., Wang, H., Huo, P. and Yan, Y. (2021). CeO_2/3D g-C_3N_4 heterojunction deposited with Pt cocatalyst for enhanced photocatalytic CO_2 reduction. *Appl. Surf. Sci*., 537, 147891. http:// doi.org/10.1016/j.apsusc.2020.147891

Zheng, S., Cai, Y. and O'Shea, K.E. (2010). TiO_2 Photocatalytic Degradation of Phenylarsonic Acid. *J. Photochem. Photobiol. A. Chem.*, 210(1), 61-68. http://doi.org/10.1016/j.jphotochem.2009.12.004

Zheng, Y., Lin, L.H., Ye, X.J., Guo, F.S. and Wang, X.C. (2014). Helical graphitic carbon nitrides with photocatalytic and optical activities. *Angew. Chem. Int. Ed*., 53(44), 11926-11930. http://doi.org/10.1002/anie.201407319

Zhou, B., Waqas, M., Yang, B., Xiao, K., Wang, S.Y., Zhu, C.Z., Li, J.Y. and Zhang, J.M. (2020a). Convenient one-step fabrication and morphology evolution of thin-shelled honeycomb-like structured g-C_3N_4 to significantly enhance photocatalytic hydrogen evolution. *Appl. Surf. Sci.*, 506, 145004. http://doi.org/10.1016/j.apsusc.2019.145004

Zhou, B.X., Ding, S.S., Zhang, B.J., Xu, L., Chen, R.S., Luo, L., Huang, W.Q., Xie, Z., Pan, A.L. and Huang, G.F. (2019a). Dimensional transformation and morphological control of graphitic carbon nitride from water-based supramolecular assembly for photocatalytic hydrogen evolution: from 3D to 2D and 1D nanostructures. *Appl. Catal. B.*, 254, 321-328. http://doi.org/10.1016/j.apcatb.2019.05.015

Zhou, C.Y., Zeng, G.M., Huang, D.L., Luo, Y., Cheng, M., Liu, Y., Xiong, W.P., Yang, Y., Song, B. and Wang, W.J. (2020b). Distorted polymeric carbon nitride via carriers transfer bridges with superior photocatalytic activity for organic pollutants oxidation and hydrogen production under visible light. *J. Hazard. Mater*., 386, 121947. http://doi.org/10.1016/j.jhazmat.2019.121947

Zhou, C.Y., Xu, P., Lai, C., Zhang, C., Zeng, G.M., Huang, D.L., Cheng, M., Hu, L., Xiong, W.P., Wen, X.F., Qin, L., Yuan, J.L. and Wang, W.J. (2019b). Rational design of graphic carbon nitride copolymers by molecular doping for visible-light-driven degradation of aqueous sulfamethazine and hydrogen evolution. *Chem. Eng. J.*, 359, 186-196. http://doi.org/10.1016/j.cej.2018.11.140

Zhou, J.J., Ji, X.H., Zhou, X.H., Guo, J., Sun, J.Y. and Liu, Y.C. (2018). Three-dimensional g-C_3N_4/MgO composites as a high-performance adsorbent for removal of Pb(II) from aqueous solution. *Sep. Sci. Technol*., 54(17), 2817-2829. http://doi.org/10.1080/01496395.2018.1553983

Zhou, L., Feng, J.R., Qiu, B.C., Zhou, Y., Lei, J.Y., Xing, M.Y., Wang, L.Z., Zhou, Y.B., Liu, Y.D. and Zhang, J.L. (2020c). Ultrathin g-C_3N_4 nanosheet with hierarchical pores and desirable energy band for highly efficient H_2O_2 production. *Appl. Catal. B*, 267, 118396. http://doi.org/10.1016/j.apcatb.2019.118396

Zhou, X.R., Zeng, Z.T., Zeng, G.M., Lai, C., Xiao, R., Liu, S.Y., Huang, D.L., Qin, L., Liu, X.G. and Li, B.S. (2020d). Persulfate activation by swine bone char-derived hierarchical porous carbon: Multiple mechanism system for organic pollutant degradation in aqueous media. *Chem. Eng. J*., 383, 123091. http://doi.org/10.1016/j.cej.2019.123091

Zhou, Y.J., Sun, L.L., Wu, D.Y., Li, X., Li, J.Z., Huo, P.W., Wang, H.Q. and Yan, Y.S. (2020e). Preparation of 3D porous g-C_3N_4 @V_2O_5 composite electrode via simple calcination and chemical precipitation for supercapacitors. *J. Alloys Compd*., 817, 152707. http://doi.org/10.1016/j.jallcom.2019.152707

Zhou, Y.J., Zhang, L.X., Liu, J.J., Fan, X.Q., Wang, B.Z., Wang, M., Ren, W.C., Wang, J., Li, M.L. and Shi, J.L. (2015). Brand new P-doped g-C_3N_4: enhanced photocatalytic activity for H_2 evolution and Rhodamine B degradation under visible light. *J. Mater. Chem.*, 3(7), 3862-3867. http://doi.org/10.1039/C4TA05292G